



UNIVERSITÀ POLITECNICA DELLE MARCHE
Repository ISTITUZIONALE

A life cycle costing of compacted lithium titanium oxide batteries for industrial applications

This is the peer reviewed version of the following article:

Original

A life cycle costing of compacted lithium titanium oxide batteries for industrial applications / Cicconi, P.; Postacchini, L.; Pallotta, E.; Monteriu, A.; Prist, M.; Bevilacqua, M.; Germani, M.. - In: JOURNAL OF POWER SOURCES. - ISSN 0378-7753. - ELETTRONICO. - 436:226837(2019), pp. 1-11. [10.1016/j.jpowsour.2019.226837]

Availability:

This version is available at: 11566/267757 since: 2022-05-30T00:55:54Z

Publisher:

Published

DOI:10.1016/j.jpowsour.2019.226837

Terms of use:

The terms and conditions for the reuse of this version of the manuscript are specified in the publishing policy. The use of copyrighted works requires the consent of the rights' holder (author or publisher). Works made available under a Creative Commons license or a Publisher's custom-made license can be used according to the terms and conditions contained therein. See editor's website for further information and terms and conditions.

This item was downloaded from IRIS Università Politecnica delle Marche (<https://iris.univpm.it>). When citing, please refer to the published version.

(Article begins on next page)

A life cycle costing of compacted Lithium Titanium Oxide batteries for industrial applications

Paolo Cicconi^{1*}, Leonardo Postacchini¹, Emanuele Pallotta¹, Andrea Monteriù¹,
Mariorosario Prist¹, Maurizio Bevilacqua¹, Michele Germani¹

¹*Università Politecnica delle Marche, via Brecce Bianche, 12, 60131, Ancona, Italy*

^{*}*Corresponding author: p.cicconi@univpm.it, tel.: +39 071 2204797*

Abstract

Nowadays, although the lithium-ion batteries have been widely applied in the context of electric vehicles for passengers, lead-acid batteries are still prevalent in motive-power applications, such as electric pallet jacks and laser guided vehicles. The battery cost is the main disadvantage that limits the employment of lithium-ion solutions in such applications. Several strategies for reducing the battery life cycle cost have been discussed in the scientific literature. The opportunity charging is one of them, even though it is suitable only for batteries having high lifecycles and high charging/discharging rates, such as the Lithium Titanium Oxide ones. This paper aims at assessing a feasible solution to reduce the life cycle cost of the energy storage units for laser guided vehicles. A tool has been proposed to analyze the Total Cost of Ownership of batteries, under the adoption of an opportunity charging strategy. Simulations of energy consumption have also been included, to predict the battery cycles and the operation costs. The life cycle analysis has investigated the use of a compacted Lithium Titanium Oxide battery in comparison with a traditional lead-acid battery. The results have shown the feasibility of the Lithium Titanium Oxide solution and its economic advantage in an industrial context.

Keywords:

Total Cost of Ownership; Li-ion batteries; LTO; Laser Guided Vehicle; Opportunity Charging.

1 Introduction

The market of Lithium-ion (Li-ion) batteries for industrial applications still concerns custom solutions. A lack of economies of scale is still evident in motive power batteries as well as in automotive [1]. The battery cost is the main factor which affects the life cycle cost of any electric vehicle. Different researchers are studying solutions focused on services, such as Vehicle-to-Grid [2], or on strategies, such as Opportunity Charging with fast-charging and downsized batteries [3].

The worldwide market of industrial batteries has a turn of about 11 billion USD [4], which regards motive power applications such forklift, Automated Guided Vehicle (AGV), Laser Guided Vehicle (LGV) and stationary systems. While Lead-Acid (LA) batteries represent the most relevant market share with 90% of MWh in 2016 [4], the turn related to the Li-ion batteries for industrial applications is less than 3 billion USD, with a market share of about 10% in terms of MWh. Even if the share of Li-ion batteries has been growing, most of the industrial batteries are still lead-acid.

Actually, most industrial Li-ion battery packs consist of Lithium Iron Phosphate (LFP) cells. Despite their high performance, LFP cells are still quite expensive; their average cost is 4-5 times the cost of the equivalent lead-acid batteries [5]. Lithium Titanium Oxide (LTO) technology is even more expensive when compared to the other Li-ion chemistries such as LFP and NMC (lithium nickel manganese cobalt oxide) [6]. However, LTO batteries can be charged and discharged at

higher C-rate [7], as highlighted in different literature reviews [6], and, due to their longer lifespan, power density [8] and safety performance [9], they are considered as an attractive energy storage solution. Moreover, LTO cells can achieve a value of power density of approximately 10 times greater than LPF cells. All these advantages are related to the use of $\text{Li}_4\text{Ti}_5\text{O}_{12}$ as anode material [10] instead of the traditional graphite [11]. This solution does not show strong ageing effects and metal plating [12]. Due to their advantages, the employment of LTO batteries in these years has started to gain a market share in fields such as Electric Vehicles [13]. In particular, these high-power density batteries can be used with Opportunity Charging [3], which refers to charging a vehicle during the operation phase, using predefined fast charging stations, avoiding full and long-time charges. Therefore, these batteries can be downsized in capacity [14].

The use of Opportunity Charging has been investigated in different research projects [15]. In one of them in particular, electric city buses with high-power charging systems have been studied [3], showing that the required high number of charging stations decreased the economic advantages of using a downsized LTO battery in buses. Opportunity Charging is often analyzed with Wireless Power Transmission (WPT) [16]. A development is represented by the dynamic wireless charging on powered roadway [17, 18, 19]. Some studies have shown that the battery range can be extended and even unlimited [20] using WPT solutions and opportunity charging. All these cases show a research interest to reduce the life cycle cost related to batteries. Regarding industrial applications, the Opportunity Charging allows a portable robot to be recharged in different stations without spending time for long-time charges and battery swapping [21]. In fact, traditional internal logistic vehicles with LA batteries require 8 h or more for charging [5].

Recently, the Li-ion technology has been earning more attention in the field of motive power, especially in the field of industrial vehicles such as LGVs [22] and AGVs [23]. These vehicles are largely used for the autonomous dispatching of loads [24], also because their dispatching and routing can be entirely controlled by a management software [22]. In this scenario, due to its properties of lightweight and long-lasting lifespan, Li-ion battery has been considered as a promising solution to power Automated Guided Vehicles [25].

This paper aims at assessing a feasible solution to reduce the life cycle cost (LCC) of energy storage units for industrial automated vehicles. The main novelty concerns the development of a design tool for an early evaluation of the battery's Total Cost of Ownership, for such motive power applications. Simulations have been conducted, since they are frequently used in literature as a research method to study operating models in different conditions [3]. A downsized LTO battery has been analyzed and compared to an LA battery in the context of LGV application with Opportunity Charging.

This paper is organized into six sections. Section 2 introduces the methodological approach for the battery's LCC, considering the modeling of battery and LGV. A test case scenario is described in Section 3, and the results are given in Section 4. Finally, Section 5 and Section 6 report the discussion and conclusions of the paper.

2 Approach

This study compares the use of LA batteries, sized to cover 8 hours of work before being swapped with a fully charged one, with the use of an LTO battery, downsized to be used with frequent charges. This last scenario involves the use of Opportunity Charging with fast charging to increase the flexibility of the system.

A simulation tool has been developed in MATLAB/Simulink® for the calculation of energy consumption and the evaluation of the battery LCC, as described in Figure 1.

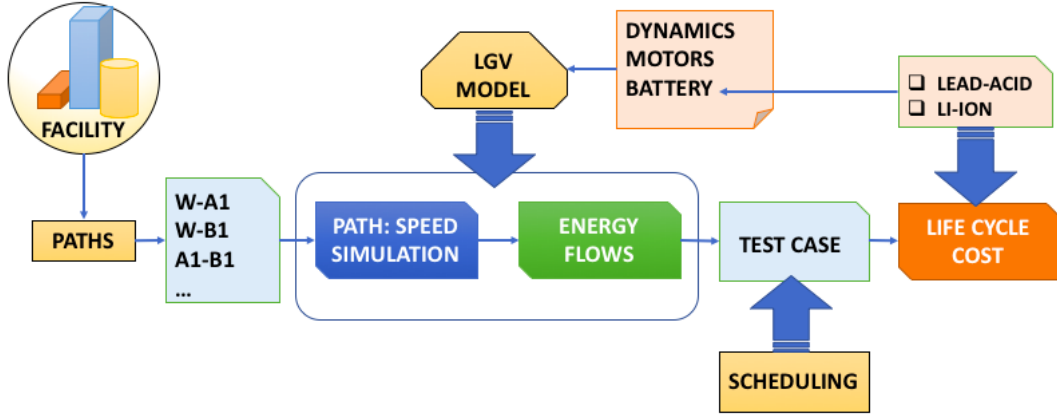


Figure 1: The proposed methodological approach.

The energy consumption of an LGV has been simulated taking into account the vehicle dynamics and the performances of motors and battery. The calculation of the LGV energy consumption depends on routes and number of dispatches. In particular, this calculation is based on three levels of analysis: definition of the speed profile, solving of the vehicle dynamics, and scheduling of all the dispatches. The energy density of the battery unit has been implicitly considered to determine the battery weight, which affects the energy consumption of any vehicles.

The speed profile has been simulated considering: an average LGV weight; the number of turns the LGV has to make; the straight paths the LGV has to drive along; the max LGV speed (1 m s^{-1}); the LGV turn speed ($0.25\text{-}0.50 \text{ m s}^{-1}$); the max LGV acceleration (0.3 m s^{-2}). The developed dynamics model also calculates the required power for the LGV driving over a defined path, considering the consumption for moving, steering, braking and auxiliaries. The electric motors related to traction and steering have been chosen and sized according to the required torque and speed. A battery model has been developed to compute the effective voltage profile and energy consumption.

2.1 Life Cycle Cost

An LCC approach is widely applied to define the TCO of batteries in electric vehicles [26], considering factors such as time and location, which affect purchasing, use, and maintaining [27]. About the ownership period, in literature, there are different examples focused on 3-years [26], 10-years [27], and 16-years period [3]. According to [27], this paper considers a 10-years period. Eq. (1) describes the calculation of the battery's TCO, which considers the *capital cost* (C_{CAP}), the *operating cost* (C_{OPE}), and the *replacement cost* (C_{REP}).

$$TCO = C_{CAP} + C_{OPE} + C_{REP} \quad (1)$$

The calculation of the capital cost (C_{CAP}) regards:

- **Battery cost:** the purchasing cost (€ kWh^{-1}) which includes the number of cells, casing, Battery Management System, etc.;
- **Charging devices cost:** the cost related to the equipment for the battery charging;
- **Swapping cost:** the LA battery requires additional automated equipment for the battery swapping. Covering 8 hours of working shift, once it is discharged, the LA battery requires to be swapped with a second fully charged one.

The annual operating costs (C_{OPE}) are related to:

- **Annual energy cost:** this cost item depends on energy consumption;

- **Annual maintenance cost:** generally, this cost is assumed to be 3% of the capital cost [3]. However, this paper does not consider any maintenance cost for batteries due to the small capacity.

Finally, the replacement cost (C_{REP}) is defined as:

- **Battery Replacement cost:** since the battery life is shorter than the vehicle's ownership period, this cost item represents the necessity to periodically substitute a battery at the end of its lifespan. In particular, a battery has to be substituted when its capacity is reduced by 20% [28]. The annualized cost for the replacing of depleted batteries is calculated at the present value.

In order to have a more practical and useful economical representation, the TCO has been discounted back to the present, using a discount rate. Therefore, the present value calculation of the Total Cost of Ownership (TCO_{pv}) has been defined as:

$$\text{Equation (2)} \quad (2)$$

where r is the discount rate, t the year of ownership, n the total years of ownership. This equation is derived from the standard equation to calculate the Net Present Value of an investment opportunity [29], but slightly modified to take into account only the annual cost invoices instead of the annual cash-flows.

The proposed LCC approach considers the following assumptions to calculate the final TCO_{pv} of a battery unit for an LGV:

1. LGV ownership is 10 years;
2. the expected lifespan for an LTO battery is 18000 cycles [30];
3. the expected lifespan for an LA battery is 1500 cycles [31];
4. an LTO battery can be fully charged in about 20 minutes (3-C rate in continuous) [30];
5. an LA battery can be charged in 8 hours;
6. the LCC analysis takes place in an industrial facility;
7. the daily energy consumption is related to a typical production scheduling. This means working on 3 shifts of 8 hours per day, 255 days a year;
8. 3% discount rate, as considered in similar studies [26] and [3].

2.2 LGV: dynamics and modeling

This section describes the analytical model applied to simulate the vehicle dynamics when an LGV vehicle is moving on a defined path. In this paper, each path is a flat indoor track with a finite number of turns and straight sections.

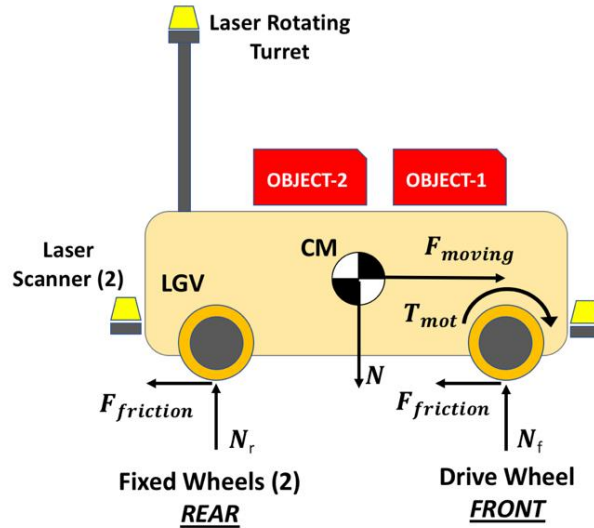


Figure 2: The simplified model of an LGV vehicle with all applied forces.

The considered LGV has three wheels. One wheel is on the front part and the remaining two wheels are on the rear part (Figure 2). The front-wheel is a drive-wheel with two electric motors for traction and steering, while the two wheels on the rear side are fixed. The total mass (m) is given by the sum of the vehicle self-weight (m_{LGV}) and the weight of the moved objects (m_{OBJ}). The analyzed LGV also has three laser-scanners. A rotating laser is applied to the LGV's turret for supporting the vehicle's navigation, by interacting with fixed reflective tapes [32]. The other two laser-scanners are used as an optical safety system to avoid accidental collisions [24].

Figure 2 describes the LGV model with all the involved forces. When the LGV is moving, the electric motor has to overcome different resistance forces, such as the ordinary ones and the accidental ones. The ordinary forces are related to wheel friction, aero drag, and floor irregularities. The accidental resistances are related to the acceleration and deceleration phases of the vehicle (uphill, downhill, obstacles, and curves). The computation of each force allows to evaluate the energy consumption.

(3)

Eq. (3) describes the sum of all the forces applied to the LGV. The drag force (F_{drag}) has been neglected in this study due to the required max indoor velocity (approximately 1 m s^{-1}). The weight force (F_{weight}) also has been neglected, due to the lack of downhill and uphill sections in this application. The resulting force to move the LGV considers the driving force (F_{moving}) and the friction force ($F_{friction}$) that is related to the normal force (N). All these forces have been described in the following formulas:

(4)

(5)

(6)

where:

m = total mass of the LGV, including battery and moved objects (kg)

m_{LGV} = mass of the LGV without battery (kg)

m_{BAT} = mass of the battery (kg)

m_{obj} = mass of the moved objects (kg)

a = acceleration ($m\ s^{-2}$)

f = friction coefficient between wheels and floor

The friction coefficient has been evaluated considering three different conditions (Table 1).

The starting phase concerns a static coefficient (f_{st}); the braking phase is characterized by a sliding friction (f_{sl}), and finally the moving phase is characterized by a rolling friction (f_{ro}), which concerns the rolling of the wheels on the floor. The friction coefficients have been provided by industrial catalogues, considering 90ShA wheels on a cement-polyurethane resin floor.

Table 1 Friction coefficients (static, sliding, rolling) for 90ShA-wheels and cement-polyurethane resin floor.

F_{st}	f_{sl}	f_{ro}
0.60	0.50	0.20

Summarizing, F_{LGV} can be simplified as follows:

$$F_{LGV} = F_{moving} + F_{Rolling} = (m_{LGV} + m_{BAT} + m_{obj}) \cdot (a + f \cdot g) \quad (7)$$

2.3 Battery modeling

2.3.1 LTO modeling

A Li-ion battery consists of several cells, which are rechargeable elements. A set of Li-ion cells can be connected with serials and parallels to define a battery pack [33]. In particular, LTO cells provide several advantages such as long life, fast charge, wide temperature range, and safety [9]. However, they are expensive and provide low specific energy, despite the high value of C-rate achievable in charging and discharging [34]. Their thermal stability is due to the lack of formation of any SEI film and lithium plating [36]. The use of LTO cells has been increasing because they can provide a lifetime between 10000 [36] and 20000 [35] cycles and even more [6].

Table 2 shows the main characteristics of typical LTO cells. Generally, they can be fast charged [37] and discharged at high C-rate [34] in continuous.

Table 2 Average values for LTO cells.

Voltages	2.30V – 2.40V nominal; typical operating range: 1.80V – 2.80V [6]; 1.50 – 2.70 [36]
Energy Density	57 [37], 70–80 [34], 89 [2] Wh kg^{-1}
Power density	2250 [38] – 2400 [6] W kg^{-1} at 50% SOC
Charge (C-rate)	1C typical; 5C maximum, 8C peak (< 1 min); charges to 2.85V

Discharge (C-rate)	4C [37], 10C possible [34], 30C 5s pulse; 1.80V cut-off
Cycle life	7000 [34], 10000 [36] [37], 15000 [39], 20000 [35] [6] [30]

Durability results for LTO cells have been analyzed by Yan *et al.* in [35]. They proposed a durability test with a temperature range between 30°C and 50°C in order to consider aging effects. They also proposed a formula (see Eq. (8)) to evaluate the equivalent cycle number related to their durability tests.

$$Cycle_e = \frac{Ah_{dch}}{Ah_{nom}} \quad (8)$$

Eq. (8) defines an equivalent cycle number ($Cycle_e$) as ratio between the total discharged energy (Ah_{dch}) per the nominal capacity (Ah_{nom}), both evaluated in Ah.

The possibility to achieve 20000 operation cycles with LTO cells has been already described in [35], together with a 20% reduction in initial capacity and a 40% increase in internal resistance. The same depletion results have been achieved after an average range of 3000 cycles for LFP cells. The proposed research is focused on LTO technology because these cells are suitable for opportunity charges at 3C rate values.

This paper considers a 20-Ah cell for the study of the LTO battery to be used in Opportunity Charging. In particular, a 20-Ah cell has been defined due to its good performance in terms of lifecycles and C-rate in charging and discharging. This cell has also been tested with a cyclor, and the experimental results have been used for modelling the equivalent RC circuit (Figure 3).

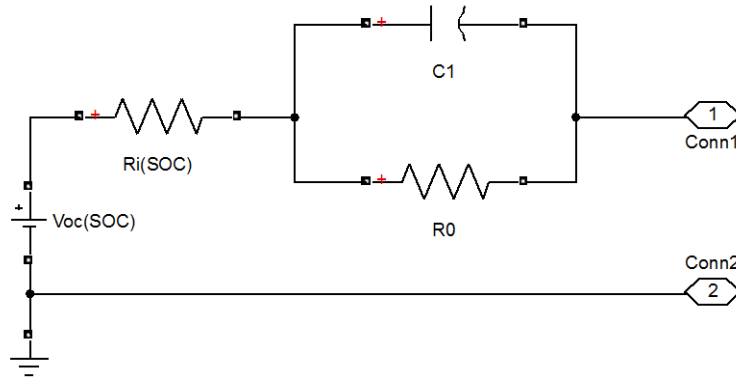


Figure 3: Equivalent circuit of a single cell.

The single cell model studied by Dubarry [40] has been used. The equivalent circuit model considers the current as the model control input and the terminal voltage as the measured output (Figure 3). The same equivalent circuit model has been analyzed in several research activities such as in [25] and [41]. This circuit consists of three parts: the equivalent ohmic internal resistor Ri ; the resistor-capacitor parallel network ($R0 // C1$), where $R0$ is the equivalent polarization resistance and $C1$ is the equivalent polarization capacitance that simulates the transient responses of the battery during charging-discharging; and the generator related to the Open Circuit Voltage, which is a nonlinear function of $SOC(t)$. Table 3 shows the main parameters used for equivalent resistances and capacitors applied in the described RC circuit (Figure 3).

Table 3: The main parameter for the equivalent RC-circuit.

Ri	R0	C1
----	----	----

1.007 mΩ	1.181 mΩ	3.486 F
----------	----------	---------

The battery SOC has been evaluated by applying Eq. (9) during the timesteps simulation, using the approach described in [42]. The resulting RC circuit has been simulated using MATLAB/Simulink®. Afterwards, the virtual model of the proposed cell has been introduced into the battery model to reproduce the battery behavior in operation. The cycle estimation has been analyzed using the cycle calculation described in Eq. (8). More details about the battery pack are described in Section 3.3.

$$SOC(t) = SOC(t_0) - \frac{1}{Q} \int_{t_0}^t i(\tau)_{discharge} d\tau \quad (9)$$

2.3.2 LA modeling

A Valve Regulated Lead-Acid (VRLA) Gel battery has been analyzed and compared with an LTO battery. Lead-Acid batteries are the most common batteries for industrial applications, due to their low purchasing cost on the market, which is the result of a consolidated manufacturing process [43]. Nowadays, several types of LA batteries are available on the market. VRLA batteries use an electrolyte gel with advantages in terms of safety, handling, absence of maintenance, and reduced emission of gases in overcharge [31]. However, this kind of batteries always require an adequate level of ventilation, because hydrogen gas is highly flammable.

Some limits related to LA batteries are highlighted in the following:

- reduced Lifetime (1500 cycles [31]);
- nonlinear charging (quick charge to 70% SOC);
- emissions of hydrogen gas.

Table 4 shows a typical datasheet for commercial 12-V modules of lead acid batteries. A lead acid battery is an array of 2-V cells [44].

Table 4 Average values for a 12-V module of a Lead Acid battery (LA).

Voltages	12 V nominal [43] (2 V per cell [44])
Energy Density	40 [31] Wh kg ⁻¹
Power density	250 [31] W kg ⁻¹
Cycle life	1500 [31]
Cost	150–200 \$ kWh ⁻¹ [31]

Here, the model proposed by Kujundžić [43] for VRLA batteries has been used as the equivalent circuit for the LA battery. This is a hybrid electrical model which considers a capacitor ($C_{capacity}$) and a current-controlled (I_{batt}) source to model the state-of-charge. The model also contains an RC network to reproduce the transient response of the battery [43]. A voltage-controlled source has been used to connect state-of-charge to an open-circuit voltage (V_{oc}).

3 Test case

This section describes the proposed test case, focusing on the battery configurations, the facility layout, and the LGV specifications. The LCC comparison is between the use of a traditional LA battery and a downsized LTO battery in opportunity charging.

The background scenario regards a facility for the production of footwear soles, inside an Italian company located in the area of Civitanova Marche. This production is affected by seasonal demand changes and therefore, manufacturing flexibility and automation are highly recommended [45]. In this context, a project called “HERCULES” [46] has been developed for 2 years to support the molds management and transportation, using a mechanized warehouse system with an automated guided vehicle [47].

3.1 LGV: the energy consumption model

The energy consumption has been calculated considering the ampere-hour losses related to each operation phase. The dispatches of a typical 1-day working scheduling have been considered. Each dispatch starts from an origin point and it ends at the assigned destination. In this route, the vehicle accelerates until it achieves its max speed (1 m s^{-1}). The LGV can maintain a constant and max speed for a straight stretch until to an intersection, a curve, or any stop condition. It decelerates before each curve and stop. While Kabir and Suzuki [5] proposed a table of ampere draws per activity, this paper simulates the dynamics of an LGV to estimate the effective energy consumption related to each dispatch. The results of the dynamics simulation (Section 2.2) are the speed profile and the force requested for moving the LGV on a defined route.

The total electric load related to the battery unit is described in Eq. (10):

$$P_{BAT}(t) = \frac{1}{\eta_{BAT}} \cdot \left(\frac{1}{\eta_{M1}} \cdot F_{LGV}(t) \cdot v(t) + \frac{1}{\eta_{M2}} \cdot P_{ste}(t) + P_{bra}(t) + P_{aux} \right) \quad (10)$$

where:

- P_{BAT} = battery electric power request (W)
- η_{BAT} = battery efficiency
- η_{M1} = motor efficiency for traction (including gear-box)
- η_{M2} = motor efficiency for steering (including gear-box)
- v = vehicle speed (m s^{-1})
- P_{ste} = power for steering (W)
- P_{bra} = power for braking (W)
- P_{aux} = power of auxiliaries (W)
- t = time (s)

As highlighted in Eq. (10), the total power load requested from the battery unit depends on different factors. The dynamics analysis gives data, such as the resistance force (F_{LGV}) defined in (7) and the speed profile (v), to compute the traction power. Other energy consumptions regard the steering motor (P_{ste}), the electromagnetic braking (P_{bra}), and the auxiliary units (P_{aux}). The auxiliaries set includes units such as laser scanners, on-board PLC, computers, general electronics boards and safety sensors. The power related to the auxiliaries has been considered as a constant. The LGV's

manufacturer indicates a nominal value of 300 W for them. Regarding the vehicle steering, the power related to the electric motor has been considered as constant during each turn and pivoting phase. The efficiency coefficients for battery and electric motors, have been set according to lookup tables.

Energy consumption has also been applied to the deceleration phase, due to the use of the electromagnetic braking in LGVs. Eq. (11) describes the calculation of the braking torque, considering the diameter of the driving wheel (D) in meters.

$$T_{bra}(t) = \frac{m \cdot D \cdot v(t)}{4 \cdot t} \quad (11)$$

Since the dynamics of the vehicle is a no-steady condition, when the vehicle is moving, Eq. (10) varies its outcome at each instant of time. The resulting energy consumption (E_{BAT}), evaluated as ampere-hour loss (Ah), has been calculated per each time-step, by multiplying the value of the ampere draw by the relative time (expressed in hours).

$$E_{BAT}(t_2 - t_1) = \int_{t_1}^{t_2} P_{BAT}(t) \cdot dt \quad (12)$$

Eq. (12) describes the energy consumption related to the battery, using the integral operator of the load power between two instants. This approach has been applied for each time-step during the vehicle simulation, in order to obtain an instant profile of the effective energy consumption.

Table 5 describes the LGV main technical specifications. This data have been analyzed together with a manufacturer of LGVs and AGVs. The direct drive unit is an AC asynchronous motor (24V, 1000W, 2300rpm) equipped with an e/m braking (5Nm, 24V).

Table 5 Technical data related to the LGV datasheet.

Property	Name	Value	Unit
LGV weight (without battery)	m_{LGV}	480	kg
Static friction coefficient	f_{st}	0.60	-
Sliding friction coefficient	f_{sl}	0.50	-
Rolling friction coefficient	f_{ro}	0.20	-
Wheel diameter (90ShA wheels)	D	220	Mm
Nominal power: 24-V direct drive motor	P_1	1000	W
Nominal rpm: 24-V direct drive motor	$N1$	2300	rpm
Nominal Torque: 24-V direct drive motor	$T1$	4,1	Nm
Gear reduction ration for driving	i_1	1:27	-
Nominal power: 24-V steering motor	P_2	150	W
Nominal rpm: 24-V steering motor	$N2$	2300	rpm
Nominal Torque: 24-V steering motor	$T2$	0.8	Nm
Gear reduction ration for steering	i_2	1:5	Nm
Max e/m braking torque	$T_{bra-max}$	5	Nm

3.2 Facility layout

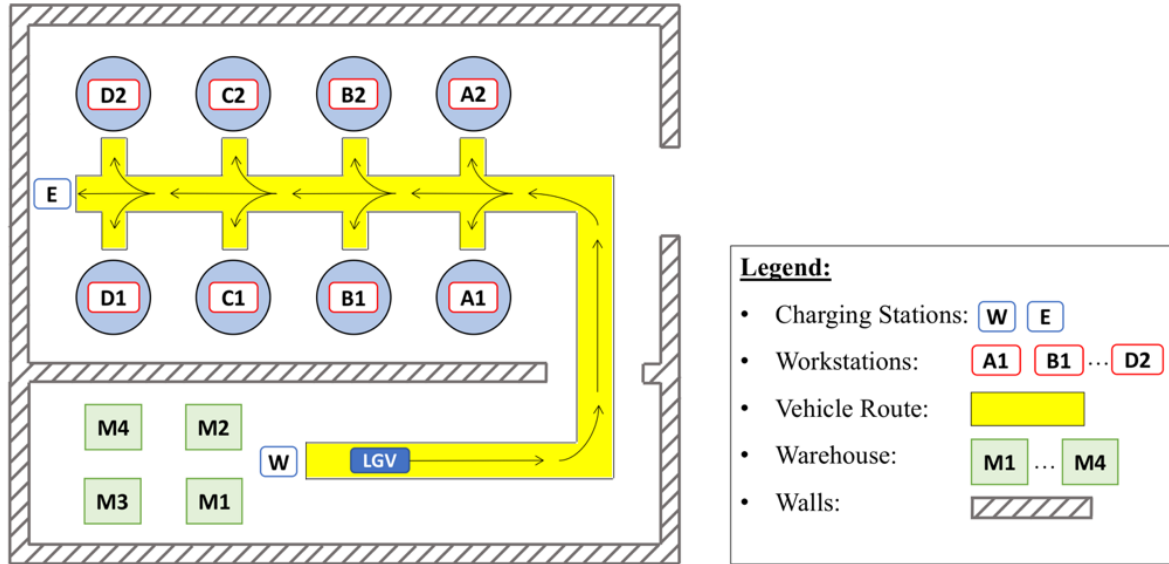


Figure 4: The facility layout.

Figure 4 shows the production layout that has been analyzed. There are 8 workstations, 2 charging stations for the LGV and 4 mechanized warehouses with molds. Each time a workstation needs to be set with a new mold, the central system receives a call and a robot picks up the mold in one of the warehouses and brings it to station W. Here is where the LGV is waiting, recharging itself (Opportunity Charging) and pending to be loaded. Once the LGV is loaded (“pick-up on W station”), it delivers the mold to the workstation. At the workstation, the LGV is firstly unloaded (“drop-off on workstation”) and then loaded back with the mold that has been replaced (“pick-up on workstation”). The LGV then moves back to the W station where it is unloaded by the robot (“drop-off on W station”). Here the LGV puts itself into a charging mode (Opportunity Charging), waiting for the next call. The LGV can transport a total of 4 pair of molds and, with proper scheduling, it can fulfill up to 4 calls with a single back and forth travel from the W station. In a normal production day (real case), each workstation calls the LGV on average once every hour and a half.

For this test case, it has been assumed that each workstation requires one (and only one) mold change every hour and the change call can happen randomly within the hour. Concerning the scheduling of the mold change, in order to cover the worst-case scenario, it has been considered a “no scheduled” situation. This means that, for each call, the LGV leaves the W station, serves the calling workstation and then comes back to the W station, even if multiple calls are already pending (likewise the LGV can transport only a single pair of molds at a time).

Within this layout, all possible LGV paths have been studied, resulting in a total of 19 different paths (see Table 6). A graph with the performance of the required LGV moving power in time has been drawn for each path, taking into account all the factors of Eq. (10). For example, Figure 5 shows the graph for the path W-A1 (equal to W-A2). An average specific consumption value has been derived to represent each particular path (in Wh m^{-1} , see Table 6).

For each path, Table 6 reports: the distance, the average energy consumption of the LGV (calculated on that particular path) and the total energy required. For instance, from workstation A

to workstation C (35 m), the LGV consumes a total of 20.30 Wh. This value has been calculated by multiplying the average specific consumption value (for that path) for the relative path distance.

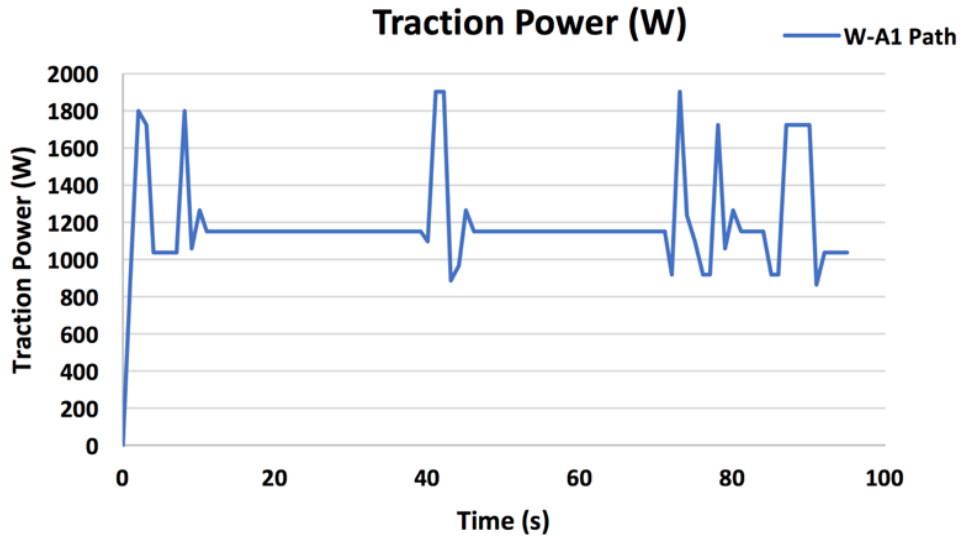


Figure 5: Traction Power related to path W-A1.

Table 6: Data and energy consumption calculated for each path.

Path	Distance (m)	Average specific consumption (Wh m ⁻¹)	Path consumption (Wh)
W-A	80	0.53	42.40
W-B	95	0.52	49.40
W-C	110	0.51	56.10
W-D	125	0.50	62.50
W-E	125	0.5	62.50
A-A	15	0.60	9.00
A-B	20	0.59	11.80
A-C	35	0.58	20.30
A-D	50	0.57	28.50
A-E	50	0.56	28.00
B-B	15	0.60	9,00
B-C	20	0.59	11.80
B-D	35	0.58	20.30
B-E	35	0.57	19.95
C-C	15	0.60	9.00
C-D	20	0.59	11.80
C-E	20	0.58	11.60
D-D	15	0.60	9.00
D-E	12	0.6	7.20

Table 7 reports the operation time (drop-off and pick-up of a mold) on the workstations and the W station.

Table 7: The considered operation for drop-off and pick-up activities.

Operation time	Drop-off time (s)	Pick-up time (s)
On a workstation	25	25
On W station	20	20

Table 8 reports the distances, the times (travelling and operational) and the power consumptions for the round-trip from W station to every single workstation. The operational and round-trip travelling time is given by the sum of the following times: pick-up time on W station, travelling time (going), drop-off time on a workstation, pick-up time on a workstation, travelling time (return) and drop-off time on W station. Table 9 shows the simulation results referred to a single operational hour.

Table 8: The dispatching description.

From W station to:	Distance (m)	Travelling time (s)		Distance round-trip (m)	Operational and round-trip travelling time (s)	Round-trip consumption (Wh)
		Going	Return			
A1	80	98	98	160	286	85
A2	80	98	98	160	286	85
B1	95	110	110	190	310	99
B2	95	110	110	190	310	99
C1	110	122	122	220	334	112
C2	110	122	122	220	334	112
D1	125	134	134	250	358	125
D2	125	134	134	250	358	125

Table 9: The report of the simulated scheduling.

Results on one operational hour	
Total distance travelled (m)	1640
Total busy time (s)	2576
Total available idle time (s)	1024
Percentage of LGV utilization	72%
Percentage of LGV idle time	28%
Total consumption (Wh)	842

The results indicate that, in order to supply all the workstation calls, the LGV consumes 842 Wh, travelling 1640 m and being busy for 2547 s out of the 3600 available. This means that, within an operational hour, the LGV has available 1024 s to recharge itself. Based on these results, the LTO battery of the LGV has been sized in 1.1 kWh capacity. With this capacity indeed, by consuming 842 Wh, this battery would reach a SOC of 23% and it would require 915 s to charge itself fully (see Table 10).

Table 10: An early estimation of the required battery performance related to one operation hour.

SOC	23%
DOD	77%
Time required for charging (s)	915

3.3 Battery

The comparison is between an LTO battery and a traditional LA one. In motive power applications, LA batteries are designed to provide energy for an operation shift of approximately 8 hours. Since for this kind of batteries a full charge requires 8 hours or more [5], a second LA battery is generally necessary.

3.3.1 LTO battery

The LTO battery has a pack configuration of 24 cells: 2 parallel lines per a series of 12 cells. The resultant battery capacity is 1104 Wh. Table 11 describes the complete battery datasheet. The selected LTO cell, which has a lithium titanium oxide in the anode layer, provides a capacity of 20 Ah [30]. The battery life has been analyzed considering the number of cycles without including an aging simulation. The aging analysis has been neglected because the manufacturer of the cells claimed a lifecycle range of 15000-20000 cycles (when the cell is continuously charged and discharged at 3C-rate [30]) and, in this study, the lifecycle span of the proposed LTO battery has been set to the intermediate value of 18000 cycles. Other cells provide similar cycles: for example, the datasheet in [39] reports a life span > 15000 cycles at 4C charge/discharge.

The sizing of the proposed LTO battery has been defined after the early study described in Section 3.2. To summarize, a 1.1-kWh battery provides the necessary energy for moving the studied LGV per 1 hour, with an acceptable remaining capacity (over 15%). Moreover, the resulting idle time per each hour shows the opportunity to recharge the battery with frequent 3-C charges.

The sizing approach has been focused on two aspects:

1. The battery capacity must provide the required energy for 1-hour operation;
2. The idle time per each hour should guarantee the time for a full fast-charging, which can be provided in frequent high C-rate charges.

Table 11: The LTO battery datasheet

Property	Value	Unit
Cell capacity	20	Ah
Cells number	24	#
Cell nominal voltage	2.3 [30]	V
Cell cycles	18000 [30]	cycles
Battery capacity	40	Ah
Battery voltage	28	V
Battery Energy	1104	Wh
Battery weight	15	kg
Module configuration	12 cells in series x 2 parallels	

The proposed approach has considered the analysis of the dynamics for the calculation of the energy consumption. Therefore, the battery simulation has evaluated SOC and energy consumption related to the velocity profile. Most of the data used for this study have been taken directly from the manufacturers of batteries and LGV. Eq.(13) describes the electrical power provided by the equivalent circuit for a generic Li-ion battery pack.

$$P_{BAT}(t) = \eta_{bat} \cdot V_{bat}(SOC) \cdot I_{bat}(t) \quad (13)$$

where:

- η_{bat} = the battery efficiency (%)
- V_{bat} = battery voltage (V), which is a function of SOC
- I_{bat} = battery current (A), which is time-dependent

3.3.2 LA battery

The simulations have compared the proposed LTO battery with a 10-kWh Lead-Acid one, considering the same scheduling scenario. The defined LA battery can provide the requested energy for the worst-case scenario with a remaining SOC of about 20% after 8 hours (28800 s). The capacity of the LA battery can overcome the load related to a working shift of 8 hours, without considering any intermediate charges. Table 12 reports data related to the LA battery, which is about 6 times heavier than the LTO one, with a capacity of more than 8 times.

Table 12: The VRLA Gel battery datasheet (LA battery).

Property	Value	Unit
Battery capacity	420	Ah
Battery voltage	24	V
Battery Energy	10	kWh
Cycles	1500	cycles
Battery weight	90	kg

3.4 Cost data

According to Section 2.1, Table 13 shows the average market cost (expressed in euro) of the items considered in this analysis. Each cost is related to the Italian market.

Regarding the cost of Li-ion batteries, several research papers have been focusing the attention on the optimal battery price for enhancing the diffusion of Li-ion batteries. Lajunen [3] considered as fair a cost of 500 € kWh⁻¹ for LFP batteries and 800 € kWh⁻¹ for LTO ones, which is a more expensive technology.

In this paper, a cost of 880 € kWh⁻¹ has been considered as the specific cost for an LTO battery. This cost includes electronics, casing, and software. This specific cost is 10% higher than the relative LTO cost exposed by Lajunen [3] due to the smaller size of the studied battery. Even though the cost of LTO cells has gone down in the recent years to values such as 500 € kWh⁻¹ in the suppliers market, the cost of casing and battery management system cannot be neglected for a 1.1-kWh battery. In the proposed battery pack, 74% of the battery cost is related to LTO cells and 26% to casing and battery management system.

Table 13: The cost items analyzed in the proposed study.

Item	Cost
LTO Battery (1,1 kWh)	970 €
LTO Charger (300 A)	1500 €
LA Battery (10 kWh)	1100 €
LA Charger	300 €
LA Swapping system	5000 €
Electricity cost	0.15 € kWh ⁻¹

Regarding the LTO charger, it has been considered a fast-charging device with a contact connection. Induction devices have not been considered, in order to completely avoid possible safety issues for the operators. A market value of € 1500 for a single LTO charger has been set for this cost analysis. A similar approach has been applied to define the cost for a typical and standard LA charger, for the Italian market, which has been set to € 300.

A specific cost of 110 € kWh⁻¹ has been set for the LA battery (VRLA-Gel type). This value has been taken from the price list of the Italian market; however, it is close to data reported in the literature [30]. Finally, a cost of € 5000 has been considered for the swapping system for LA batteries.

4 Results

Figure 6 describes the simulated current profile using the proposed LTO battery with Opportunity Charging. The resulting profiles of charging and discharging have been highlighted with different colors. The red line is the discharging current profile, which is related to 1-h operation. The blue

line is the profile related to the opportunity charging. The resulting profile of the battery current is the sum between the two current profiles in charging and discharging. Each dispatch is a round-trip that reduces the battery capacity of about 10%. The use of opportunity charging can fill the battery at each stop at the W-station.

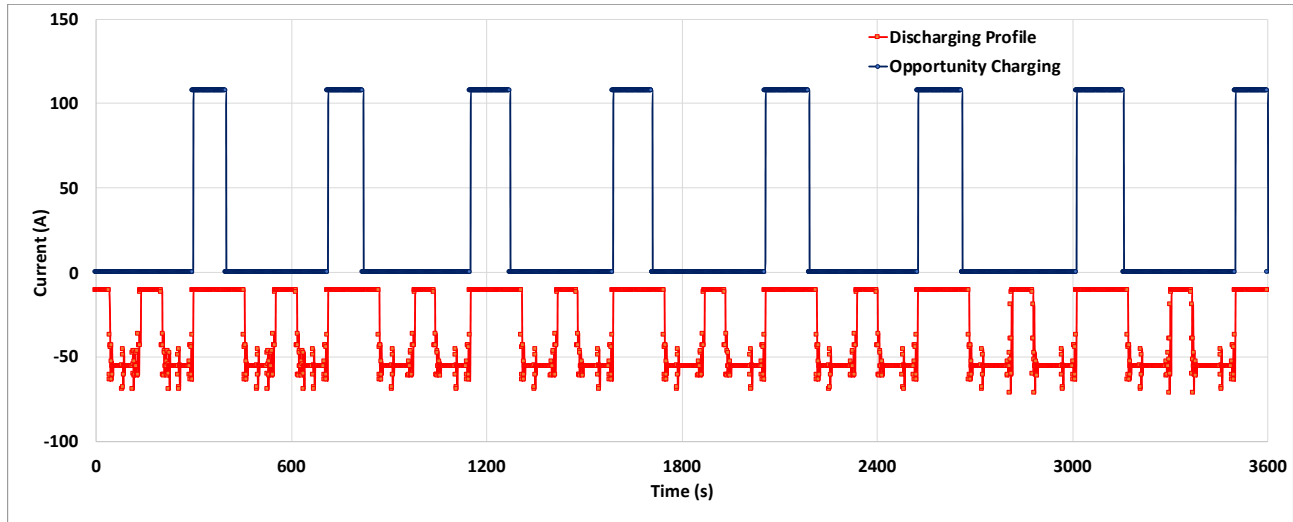


Figure 6: The comparison between the discharging profile due to the LGV operation (red line) and the current profile related to the Opportunity Charging (blue line).

Figure 7 shows the energy comparison of the two different battery technologies in terms of a single round-path (W-A1 path). Even though the described energy profiles are similar, the LA battery shows a higher consumption due to its less efficiency and more weight.

Figure 8 shows the SOC profile for two operation cases, respectively with and without Opportunity Charging for the LTO battery. This result is related to the same scheduling scenario, previously defined. While the blue line reports the SOC decreasing for 1-h operation without any intermediate charge, the red line describes the SOC profile using the opportunity charging. In particular, each charge is performed during each stop at W-workstation. Without these charges, the battery SOC decreases up to 16% (Figure 8, blue line). Moreover, a battery swapping or at least a long charging pause should be scheduled if the Opportunity Charging is not considered for a such downsized battery. Therefore, the Opportunity Charging allows the battery to achieve the maximum level of SOC before each dispatch.

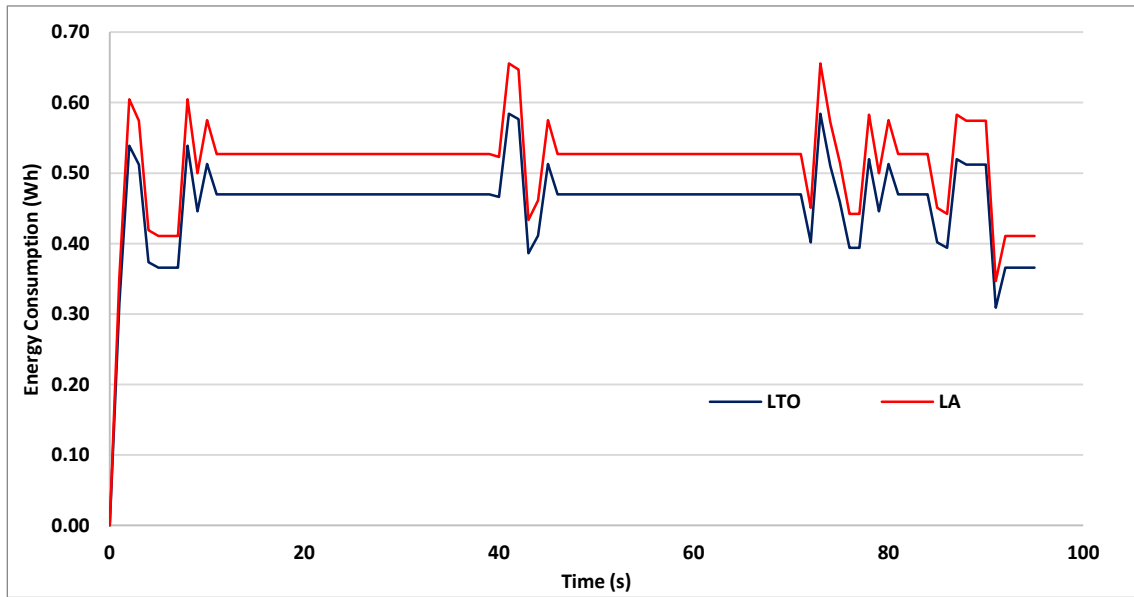


Figure 7: Energy consumption: the comparison between the use of LTO (dark blue line) and LA (red line) batteries for the W-A1 path.

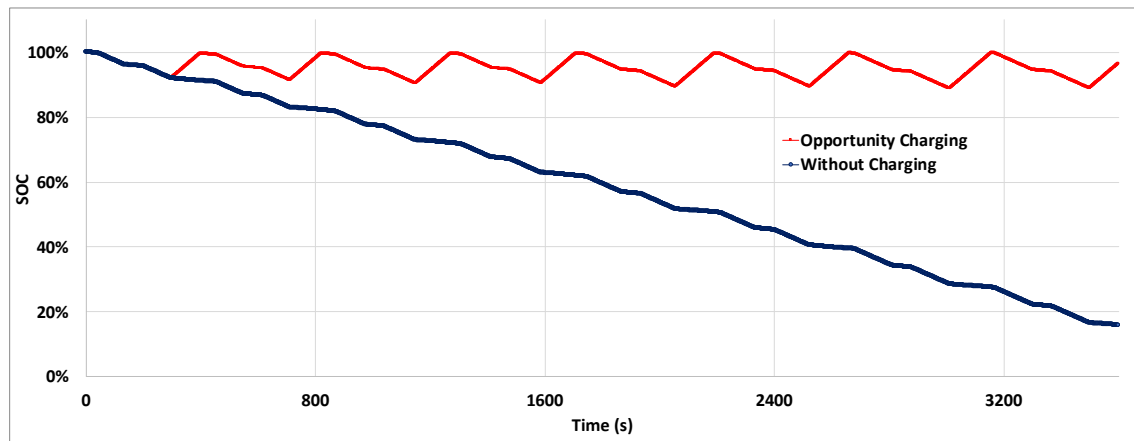


Figure 8: The comparison between the SOC profile with the “opportunity charging” (red line) and without charging (dark blue line) the battery during 1-h operation.

4.1 LCC

Table 14 reports the results of the LCC analysis for the two different battery systems over ten years of ownership. For the LTO battery system, the “LTO charger” invoice of the first year (year 0 in the table) is equal to 3000 € due to the purchasing of two chargers (one for the W station and one for the emergency charge station E). For the LA battery system, the “LA battery” invoice is 2000 € every single time, due to the need of purchasing a couple of batteries. Indeed, this battery system requires that, while a battery is working for a day shift, the other one is charging to be ready to work the next shift. When a battery is working the other is charging and vice versa. The LTO battery must be replaced every 4 years. This has been calculated considering the assumptions made in Section 2.1. In this test case, indeed, the LTO battery needs approximately 4651 recharge cycles a year. The LA batteries must be replaced every 4 years as well. In this test case, indeed, the single LA battery needs approximately 390 recharge cycles a year. The actualized Total Cost of Ownership (TCO_{pv}) has been obtained using Eq. (2).

Table 14: Result of the LCC analysis.

Cost invoice	0	1	2	3	4	5	6	7	8	9
LTO battery	970 €				970 €				970 €	
LTO charger	3000 €									
LTO Consumptions	780 €	780 €	780 €	780 €	780 €	780 €	780 €	780 €	780 €	780 €
LTO TCO_{pv}	4750 €	5507 €	6243 €	6956 €	8511 €	9184 €	9837 €	10471 €	11853 €	12451 €
LA battery	2200 €				2200 €				2200 €	
LA charger	300 €									
LA swapping system	5000 €									
LA Consumptions	858 €	858 €	858 €	858 €	858 €	858 €	858 €	858 €	858 €	858 €
LA TCO_{pv}	8358 €	9191 €	10000 €	10785 €	13502 €	14242 €	14961 €	15658 €	18072 €	18730 €

The LCC analysis shows LTO technology being able to cut down consistently the actualized TCO when compared to LA technology. In this test case, the TCO_{pv} of the LTO battery shows a reduction of approximately 33% the TCO_{pv} of LA, passing from 18730 € to 12451 €. This is due to a saving in the annual electric consumption, of approximately 10%, together with a no need to purchase a battery swapping system for the LTO technology. This also means a substantial cut in the capital equipment cost for the LTO technology (approximately 43%), from 8358 € to 4750 €, if compared with the LA battery. Moreover, both the battery technologies have shown analogous lifespan but, while the LTO technology requires each time the replacement of a single battery unit, the LA technology requires a pair of batteries (doubling the cost).

The LTO battery, with Opportunity Charging, has resulted not only to be preferable in terms of Total Cost of Ownership, but also more versatile in the use. This is due to the fact that the LTO technology can be charged and discharged in continuous at high C-rate. It is the possibility of the fast-charging for LTO cells that enhances the “Opportunity Charging” benefits.

5 Discussion

This research has dealt with the use of a compacted LTO battery for motive power applications and it has provided a tool which implements a methodological approach for batteries' TCO analysis. The use of a compacted battery has involved the study of a small energy storage unit, downsized in capacity. However, the use of such solution increases the number of the required battery cycles per each working day. The LTO technology has been selected for its characteristic to be charged at higher C-rate, providing an elevate number of lifecycles. Due to this fact, other Li-ion solutions, such as LFP, NMC and LCO (Lithium Cobalt Oxide), have not been considered in this study. The drawbacks which limit the use of LFP, NMC and LCO cells are low power density and reduced C-rate in charging when compared to LTO. In particular, LCO cells, which are widely used in electronic devices for their energy density [48], are not used in vehicle applications due to their low power density, temperature issue, and the high cost of Cobalt [49].

The energy density is an important characteristic for every battery. In particular, Li-ion cells provide a good value of energy density when compared to LA solutions. In this study, the selection of the battery cells has not been limited to the energy density. Indeed, a great relevance has been given to the evaluation of the power density and the C-rate values which can be supported in continuous charging and discharging. Since the energy density affects the battery's weight, this

1 quantity has been implicitly considered in the calculation of the energy consumption when the LGV
2 is moving. However, the employment of a downsized battery reduces the weight related to a full-
3 capacity battery.

4 In the context of Industry 4.0, this paper has shown a solution to reduce the inefficiency and the
5 cost, related to the battery charging and swapping for automated guided vehicles. The possibility of
6 frequent and rapid charging along the LGV's route increases flexibility and autonomy. The
7 opportunity charging can be applied in specific stations during phases where the vehicle is stopped
8 for loading or unloading.
9

10 Regarding the implementation of such compacted LTO batteries in industrial vehicles, some design
11 risks should be considered. The main design risks concern the weight balance in some situations. In
12 fact, vehicles such as forklifts or similar, need a detailed design of the center-of-mass and self-
13 weight, in order to guarantee balance in each condition and avoid overturning when the load is
14 moving. Since the use of a compacted LTO battery instead of a lead-acid one can bring to a weight
15 reduction of approximately 50-80 kg, a ballast weight has to be considered for industrial vehicles
16 with lifting.
17

18 Another discussion regards the volume of the battery holder. In fact, the battery downsizing leads to
19 a reduction in the required battery chamber. Therefore, there is an allocable space for the
20 installation of a battery cooling system, which could enhance the performance and the health of the
21 involved Li-ion cells.
22

23 As aforementioned, nowadays the lead-acid technology represents the most used industrial battery
24 in the worldwide market [4], due to its economic advantages. Having shown the possibility of a
25 consistent cost saving, obtained through the adoption of a downsized and compacted LTO battery
26 together with the use of Opportunity Charging, the findings of this paper could affect and reverse
27 this actual trend.
28

29 Several literature reviews describe a lifespan range between 15000-20000 cycles for LTO cells, as
30 highlighted in [6, 30, 35, 36, 37, 39]. Recently, LTO manufacturers also affirm the possibility to
31 use an LTO cell at 4 C-rate charge/discharge for 15000 cycles [39]. Therefore, this paper has
32 considered a lifespan of 18000 cycles for LTO cells, using 3-C rate in charging and 1-C rate in
33 discharging. Even though today LTO cells are more expensive, several marketing forecasts show an
34 upcoming cost reduction rated of 5% by year [4]. Therefore, the LTO batteries could be more
35 convenient in the very next future and the TCO analysis proposed in this paper confirms this trend
36 for an industrial application.
37
38
39
40
41
42
43
44

45 6 Conclusions

46 In this paper, a specific tool has been described and proposed in order to analyze the life cycle cost
47 of batteries for motive power applications. In order to evaluate the battery State-of-Charge and its
48 cycles, a simplified equivalent circuit has been modelled. In particular, the test case has regarded
49 the comparison between an LA battery and an LTO battery, in an LGV application. A vehicle
50 model has been defined and simulated in order to evaluate the energy consumption related to each
51 LGV dispatching, considering all the resistance forces, the efficiencies, and the auxiliary loads.
52 Therefore, this paper has also dealt with the study of the energy consumption for moving an LGV
53 inside a facility layout. Although the simulation has been focused on a motive power application,
54 the proposed tool can be easily extended and applied in other different contexts (such as the
55 automotive context).
56

57 The proposed study has been focused on a footwear company, which produces soles for shoes. This
58 scenario has considered a worst-case analysis for the dispatching of molds from mechanized
59
60
61
62
63
64
65

warehouses to molding machines. In particular, the worst-case scenario has considered 8 dispatches per hour, with the possibility of recharging the LGV battery at the main station during the handling phases.

Summarizing, the test case has described a technical and a life cycle cost approach to evaluate the feasibility of the use of a compacted LTO battery, together with Opportunity Charging, in the context of laser guided vehicles for Industry 4.0. The LTO technology has been selected due to its characteristic to be charged and discharged in continuous at 3 or 4 C-rate with a good lifespan. The performance and cost of the configured LTO battery have been compared with a traditional lead-acid battery. While the LTO battery has achieved a capacity of 1.1 kWh using 20-h cells, the LA battery (a VRLA Gel battery) has required a capacity of 10 kWh. The scenario with the LA technology had considered the use of two batteries, which require to be swapped after each working shift. On the contrary, in the scenario with the LTO battery, a single battery is required. The results of the comparison have highlighted that the use of a compacted LTO battery, for industrial applications, can be a suitable solution in terms of technical and economic feasibility.

A TCO analysis has been used to evaluate the two different life cycle scenarios. The results have shown that using a downsized LTO battery with Opportunity Charging is more convenient than a traditional lead-acid system. The cost saving has been approximately of 33%, considering the actualized LCC values. The cost reduction is related to the possibility to avoid the purchase of a secondary battery for swapping; therefore, the purchase of the swapping system itself is not present in the LTO scenario. Moreover, an additional cost saving is related to the purchase of a compacted LTO battery. In fact, although their specific cost (€ kWh^{-1}) is higher than the specific cost of LA batteries, the downsizing in their capacity leads to a lower final battery cost. The LTO technology can also provide a lifespan of about 10 times longer than a traditional lead-acid battery.

As a future development, the proposed life cycle tool could include an environmental Life Cycle Assessment. This in order to compare the cost advantages with the possible environmental loads, due to the particular selected battery materials and the battery manufacturing process itself. A further reduction of the battery capacity could also be evaluated, considering other additional charging points and an optimized scheduling for the LGV dispatching. Moreover, the battery simulation could include an aging analysis and an analytical temperature evaluation, in order to evaluate a more reliable lifecycle for the LTO cells. Finally, the inductive fast-charging has not been analyzed in this paper and it should be analyzed in further work.

Acknowledgments

This work is part of an Italian project called HERCULES (*High Efficiency and compact eneRgy storage solutions for multi-function laser guided vehicles Controlled and monitored Using smart ICT LEan-logistics solutionS*), namely POR-FESR 2014-2020 Project n. 15351. This project is funding by REGIONE MARCHE in the context of POR FESR, which is an Italian research framework. The authors would like to thank all business partners.

Nomenclature

AGV: Automated Guided Vehicles

DOD: Depth Of Discharge

LA: Lead-Acid

LCC: Life Cycle Cost

LFP: LiFePO_4 - Lithium Iron Phosphate

LGV: Laser Guided Vehicle

LTO: Lithium Titanium Oxide

SOC: State of Charge

VRLA: Valve Regulated Lead-Acid

References

- [1] R. Bohnsack, J. Pinkse, and A. Kolk, "Business models for sustainable technologies: Exploring business model evolution in the case of electric vehicles," *Research Policy*, vol. 43, no. 2, pp. 284–300, Mar. 2014.
- [2] A.W. Thomson, "Economic implications of lithium ion battery degradation for Vehicle-toGrid (V2X) services", *Journal of Power Sources*, 396, pp. 691-709, Aug. 2018.
- [3] A. Lajunen, "Lifecycle costs and charging requirements of electric buses with different charging methods," *Journal of Cleaner Production*, vol. 172, pp. 56–67, Jan. 2018.
- [4] C. Pillot, The rechargeable battery market and main trends 2014–2025, 33rd International Battery Seminar & Exhibit, March 20th, 2017, Fort Lauderdale, FL, USA.
- [5] Q. S. Kabir and Y. Suzuki, "Increasing manufacturing flexibility through battery management of automated guided vehicles," *Computers & Industrial Engineering*, vol. 117, pp. 225–236, Mar. 2018.
- [6] R. Wegmann, V. Döge, and D. U. Sauer, "Assessing the potential of a hybrid battery system to reduce battery aging in an electric vehicle by studying the cycle life of a graphite|NCA high energy and a LTO|metal oxide high power battery cell considering realistic test profiles," *Applied Energy*, vol. 226, pp. 197–212, Sep. 2018.
- [7] K. Zaghib, M. Dontigny, A. Guerfi, P. Charest, I. Rodrigues, A. Mauger, and C. M. Julien, "Safe and fast-charging Li-ion battery with long shelf life for power applications," *Journal of Power Sources*, vol. 196, no. 8, pp. 3949–3954, Apr. 2011.
- [8] M. R. Giuliano, A. K. Prasad, and S. G. Advani, "Experimental study of an air-cooled thermal management system for high capacity lithium–titanate batteries," *Journal of Power Sources*, vol. 216, pp. 345–352, Oct. 2012.
- [9] K. Wang, F. Gao, Y. Zhu, H. Liu, C. Qi, K. Yang, and Q. Jiao, "Internal resistance and heat generation of soft package $\text{Li}_4\text{Ti}_5\text{O}_{12}$ battery during charge and discharge," *Energy*, vol. 149, pp. 364–374, Apr. 2018.
- [10] L. Zhang, S. Zhang, Q. Zhou, K. Snyder, and T. Miller, "Electrolytic solvent effects on the gassing behavior in LCO||LTO batteries," *Electrochimica Acta*, vol. 274, pp. 170–176, Jun. 2018.
- [11] Y. Cao, Q. Li, S. Lou, Y. Ma, C. Du, Y. Gao, and G. Yin, "Enhanced electrochemical performance of $\text{Li}_4\text{Ti}_5\text{O}_{12}$ through in-situ coating 70Li₂S-30P₂S₅ solid electrolyte for all-solid-state lithium batteries," *Journal of Alloys and Compounds*, vol. 752, pp. 8–13, Jul. 2018.

- [12] R. Wegmann, V. Döge, and D. U. Sauer, "Assessing the potential of an electric vehicle hybrid battery system comprising solid-state lithium metal polymer high energy and lithium-ion high power batteries," *Journal of Energy Storage*, vol. 18, pp. 175–184, Aug. 2018.
- [13] X. Feng, M. Ouyang, X. Liu, L. Lu, Y. Xia, and X. He, "Thermal runaway mechanism of lithium ion battery for electric vehicles: A review," *Energy Storage Materials*, vol. 10, pp. 246–267, Jan. 2018.
- [14] Z. Bi, T. Kan, C. C. Mi, Y. Zhang, Z. Zhao, and G. A. Keoleian, "A review of wireless power transfer for electric vehicles: Prospects to enhance sustainable mobility," *Applied Energy*, vol. 179, pp. 413–425, Oct. 2016.
- [15] Bailey JR, Hairr ME. Wayside charging and hydrogen hybrid bus: extending the range of electric shuttle buses. Washington, DC: U.S. Department of Transportation Federal Transit Administration; 2012.
- [16] S. Taghizadeh, M. J. Hossain, J. Lu, and W. Water, "A unified multi-functional on-board EV charger for power-quality control in household networks," *Applied Energy*, vol. 215, pp. 186–201, Apr. 2018.
- [17] C. C. Mi, G. Buja, S. Y. Choi, and C. T. Rim, "Modern Advances in Wireless Power Transfer Systems for Roadway Powered Electric Vehicles," *IEEE Transactions on Industrial Electronics*, vol. 63, pp. 6533–6545, 2016.
- [18] P. Venugopal, A. Shekhar, E. Visser, N. Scheele, G. R. Chandra Mouli, P. Bauer, and S. Silvester, "Roadway to self-healing highways with integrated wireless electric vehicle charging and sustainable energy harvesting technologies," *Applied Energy*, vol. 212, pp. 1226–1239, Feb. 2018.
- [19] Morris C. The dynamic road ahead: Utah State University builds the nation's most advanced test facility for dynamic wireless charging. Charged EVs: <chargedevs.com>; Nov/Dec 2014. p. 82–7.
- [20] Miller JM, Jones PT, Li J-M, Onar OC. ORNL experience and challenges facing dynamic wireless power charging of EV's. *IEEE Circ Syst Mag*; 2015. p. 40–53.
- [21] B. Zou, X. Xu, Y. (Yale) Gong, and R. De Koster, "Evaluating battery charging and swapping strategies in a robotic mobile fulfillment system," *European Journal of Operational Research*, vol. 267, no. 2, pp. 733–753, Jun. 2018.
- [22] A. Ferrara, E. Gebennini, and A. Grassi, "Fleet sizing of laser guided vehicles and pallet shuttles in automated warehouses," *International Journal of Production Economics*, vol. 157, pp. 7–14, Nov. 2014.
- [23] G. Vasiljević, D. Miklić, I. Draganjac, Z. Kovačić, and P. Lista, "High-accuracy vehicle localization for autonomous warehousing," *Robotics and Computer-Integrated Manufacturing*, vol. 42, pp. 1–16, Dec. 2016.
- [24] M. Raineri, S. Perri, and C. G. L. Bianco, "Online velocity planner for Laser Guided Vehicles subject to safety constraints," 2017 IEEE/RSJ International Conference on Intelligent Robots and Systems (IROS), Sep. 2017.

[25] Liu, Xiangyong, Wanli Li, and Aiguo Zhou. "PNGV Equivalent Circuit Model and SOC Estimation Algorithm for Lithium Battery Pack Adopted in AGV Vehicle." *IEEE Access* 6 (2018): 23639-23647.

[26] K. Palmer, J. E. Tate, Z. Wadud, and J. Nellthorp, "Total cost of ownership and market share for hybrid and electric vehicles in the UK, US and Japan," *Applied Energy*, vol. 209, pp. 108–119, Jan. 2018.

[27] A. Rusich and R. Danielis, "Total cost of ownership, social lifecycle cost and energy consumption of various automotive technologies in Italy," *Research in Transportation Economics*, vol. 50, pp. 3–16, Aug. 2015.

[28] P. Cicconi, D. Landi, A. Morbidoni, and M. Germani, "Feasibility analysis of second life applications for Li-Ion cells used in electric powertrain using environmental indicators," 2012 IEEE International Energy Conference and Exhibition (ENERGYCON), Sep. 2012.

[29] J. V. Farr, "Systems Life Cycle Costing," CRC Press, Jun. 2011.

[30] Toshiba, SCiB™ Cells - High energy 20Ah cell, *SCiB™ Rechargeable Battery*. <https://www.scib.jp/en/download/ToshibaRechargeableBattery-en.pdf> (accessed 10 June 2019)

[31] G. J. May, A. Davidson, and B. Monahov, "Lead batteries for utility energy storage: A review," *Journal of Energy Storage*, vol. 15, pp. 145–157, Feb. 2018.

[32] B. Massimo, B. Luca, B. Alberto, and C. Alessandro, "A Smart vision system for advanced LGV navigation and obstacle detection," 2012 15th International IEEE Conference on Intelligent Transportation Systems, Sep. 2012.

[33] P. Cicconi, D. Landi, and M. Germani, "Thermal analysis and simulation of a Li-ion battery pack for a lightweight commercial EV," *Applied Energy*, vol. 192, pp. 159–177, Apr. 2017.

[34] L. Ianniciello, P. H. Biwolé, and P. Achard, "Electric vehicles batteries thermal management systems employing phase change materials," *Journal of Power Sources*, vol. 378, pp. 383–403, Feb. 2018.

[35] D. Yan, L. Lu, Z. Li, X. Feng, M. Ouyang, and F. Jiang, "Durability comparison of four different types of high-power batteries in HEV and their degradation mechanism analysis," *Applied Energy*, vol. 179, pp. 1123–1130, Oct. 2016.

[36] H. Hesse, M. Schimpe, D. Kucevic, and A. Jossen, "Lithium-Ion Battery Storage for the Grid—A Review of Stationary Battery Storage System Design Tailored for Applications in Modern Power Grids," *Energies*, vol. 10, no. 12, p. 2107, Dec. 2017.

[37] F. Hall, J. Touzri, S. Wußler, H. Buqa, and W. G. Bessler, "Experimental investigation of the thermal and cycling behavior of a lithium titanate-based lithium-ion pouch cell," *Journal of Energy Storage*, vol. 17, pp. 109–117, Jun. 2018.

[37] J. Jaguemont, N. Omar, F. Martel, P. Van den Bossche, and J. Van Mierlo, "Streamline three-dimensional thermal model of a lithium titanate pouch cell battery in extreme temperature conditions with module simulation," *Journal of Power Sources*, vol. 367, pp. 24–33, Nov. 2017.

[39] Leclanché, Lithium Ion technology, *Technology & Products*. <https://www.leclanche.com/wp-content/uploads/2019/04/LECLANCHE-LECCELL-ITOWeb.pdf> (accessed 10 June 2019)

[40] M. Dubarry, N. Vuillaume, and B. Y. Liaw, "From single cell model to battery pack simulation for Li-ion batteries," *Journal of Power Sources*, vol. 186, no. 2, pp. 500–507, Jan. 2009.

[41] D. Mu, J. Jiang, and C. Zhang, "Online Semiparametric Identification of Lithium-Ion Batteries Using the Wavelet-Based Partially Linear Battery Model," *Energies*, vol. 6, no. 5, pp. 2583–2604, May 2013.

[42] T. Huria, M. Ceraolo, J. Gazzarri, and R. Jackey, "High fidelity electrical model with thermal dependence for characterization and simulation of high power lithium battery cells," *IEEE International Electric Vehicle Conference*, Mar. 2012.

[43] G. Kujundžić, Š. Ileš, J. Matuško, and M. Vašak, "Optimal charging of valve-regulated lead-acid batteries based on model predictive control," *Applied Energy*, vol. 187, pp. 189–202, Feb. 2017.

[44] A.-I. Stan, M. Swierczynski, D.-I. Stroe, R. Teodorescu, S. J. Andreassen, and K. Moth, "A comparative study of lithium ion to lead acid batteries for use in UPS applications," *2014 IEEE 36th International Telecommunications Energy Conference (INTELEC)*, Sep. 2014.

[45] B. Ulutas and A. A. Islier, "Dynamic facility layout problem in footwear industry," *Journal of Manufacturing Systems*, vol. 36, pp. 55–61, Jul. 2015.

[46] P. Cicconi, A. C. Russo, M. Germani, M. Prist, E. Pallotta, and A. Monteriù, "Cyber-physical system integration for industry 4.0: Modelling and simulation of an induction heating process for aluminium-steel molds in footwear soles manufacturing," *2017 IEEE 3rd International Forum on Research and Technologies for Society and Industry (RTSI)*, Sep. 2017.

[47] L. Cavanini, P. Cicconi, A. Freddi, M. Germani, S. Longhi, A. Monteriù, E. Pallotta and M. Prist, "A preliminary study of a Cyber Physical System for Industry 4.0: Modelling and Co-Simulation of an AGV for smart factories," *IEEE International Workshop on Metrology For Industry 4.0 and IoT*, April 2018.

[48] J. Lim, A. Choi, H. Kim, S. W. Doo, Y. Park, and K. T. Lee, "In situ electrochemical surface modification for high-voltage LiCoO₂ in lithium ion batteries," *Journal of Power Sources*, vol. 426, pp. 162–168, Jun. 2019.

[49] M. Hu, X. Pang, and Z. Zhou, "Recent progress in high-voltage lithium ion batteries," *Journal of Power Sources*, vol. 237, pp. 229–242, Sep. 2013.